Supplementary Materials

Synthesis and Controllable Oxidation of Monodisperse Cobalt-Doped Wüstite Nanoparticles and their Core-Shell Stability and Exchange-Bias Stabilization

Chih-Jung Chen,[a,b] *Ray-Kuang Chiang,* [*a] *Saeed Kamali,* [*c] *and Sue-Lein Wang*[b]

[a] Nanomaterials Laboratory, Far East University, Hsing-Shih, Tainan 74448, Taiwan
[b] Department of Chemistry, National Tsing Hua University, Hsinchu 30013, Taiwan
[c] MABE Department, University of Tennessee Space Institute, Tullahoma, TN 37388, USA

*Correspondence should be addressed to rkc.chem@msa.hinet.net and skamail@utsi.edu

Table S1. Structural parameters of 12.5 nm and 19 nm 20h-oxidized Co-doped FeO NPs.

Diameters (nm)	Core diameter (nm)	Shell thickness (nm)	Core volume (nm^3)	Shell volume (nm^3)	Shell-to-core volume ratio
12.5	4.5	4	91	1862	20.4
19	11	4	1331	5528	4.2

Table S2. Magnetic parameters of 12.5 nm and 19 nm 20h-oxidized Co-doped FeO NPs.

Size / Temp.	12.5 nm			19 nm		
	H_E (Oe)	V_S (emu/g)	FC-H_C (Oe)	H_E (Oe)	V_S (emu/g)	FC-H_C (Oe)
5 K	4302	2.11	13754	2500	6.3	16096
100 K	290	0.89	1896	644	1.12	9917
150 K	10	0.02	1204	169	0.36	6024
200 K	0	0	415	36	0.16	3346
250 K	0	0	312	0	0	1350
300 K	0	0	0	0	0	601

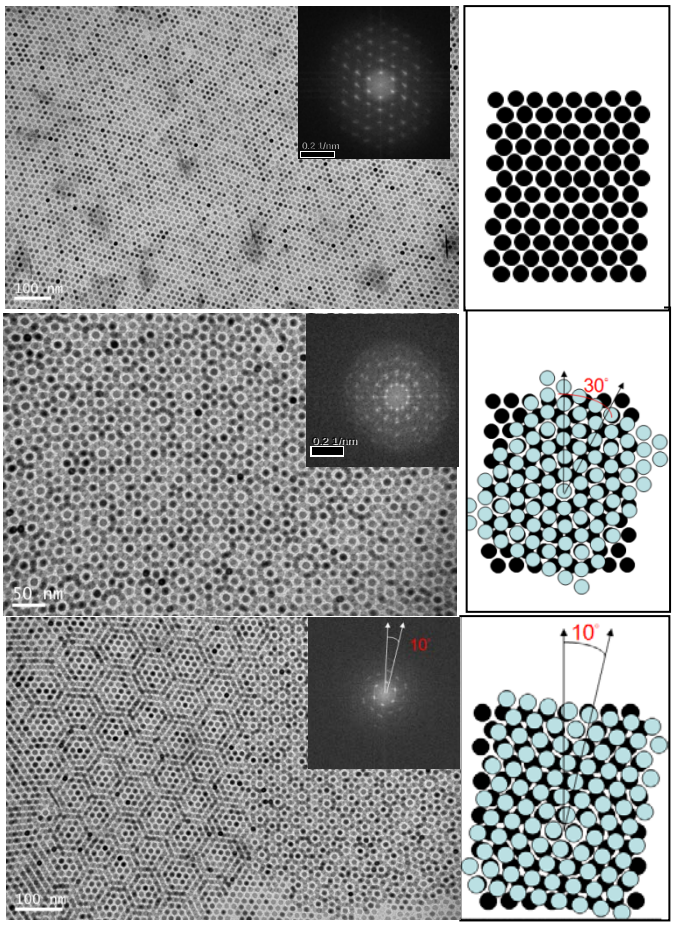

Fig. S1. A typical multi-layered hexagonal-close-packed structure of CWT NPs.

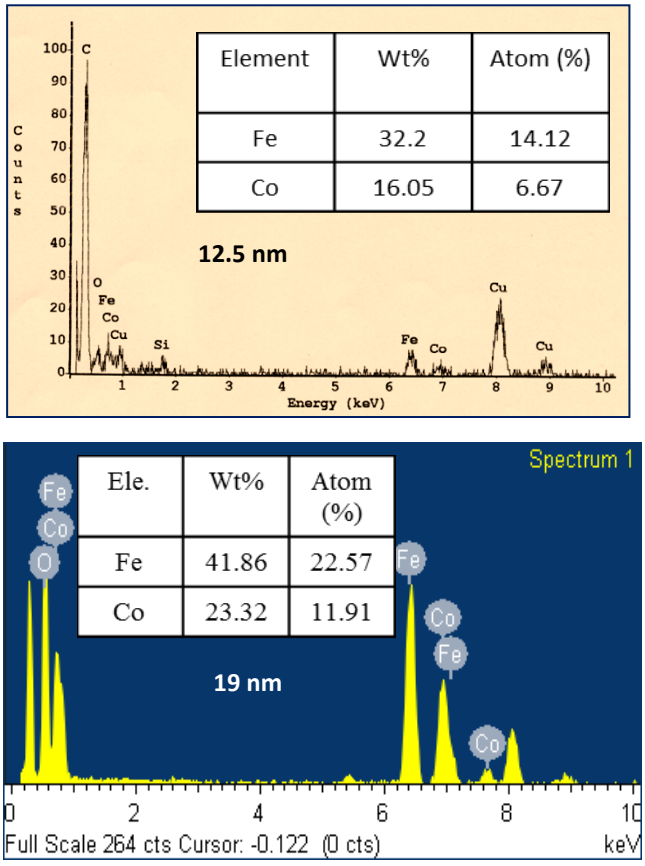

Fig. S2. The elemental analysis of cobalt in the CWT NPs and showed the Fe-to-Co ratio to be around 2:1 by ICP for the NP product with a size of 12.5 nm and 19 nm.respectively.

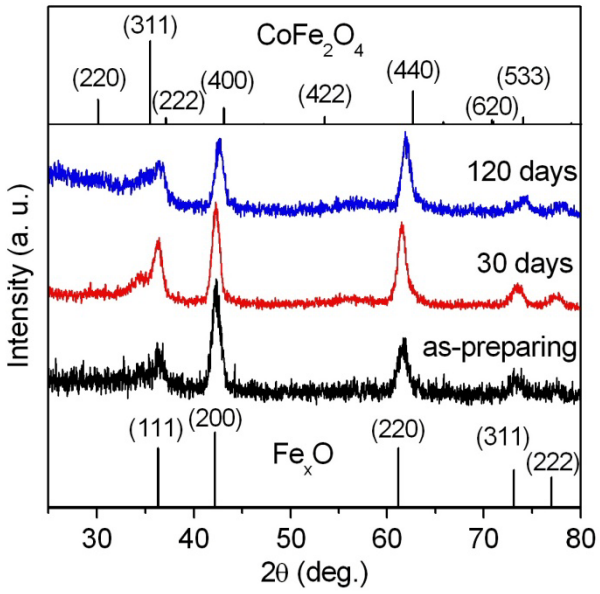

Fig. S3. XRD patterns of products of ambient oxidation.

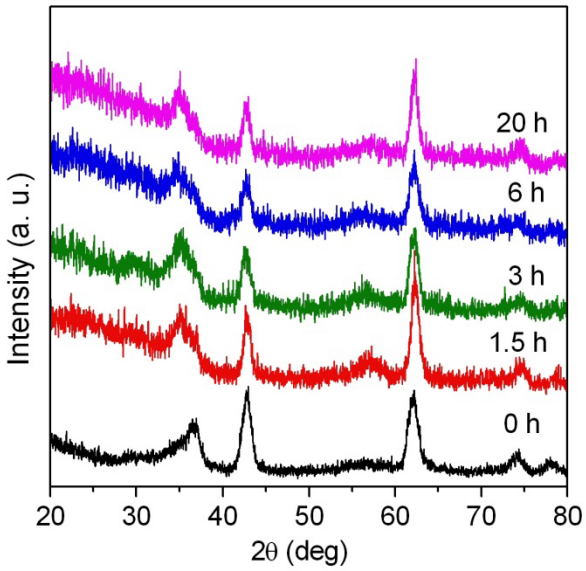

Fig. S4. XRD patterns of products of expedited oxidation.

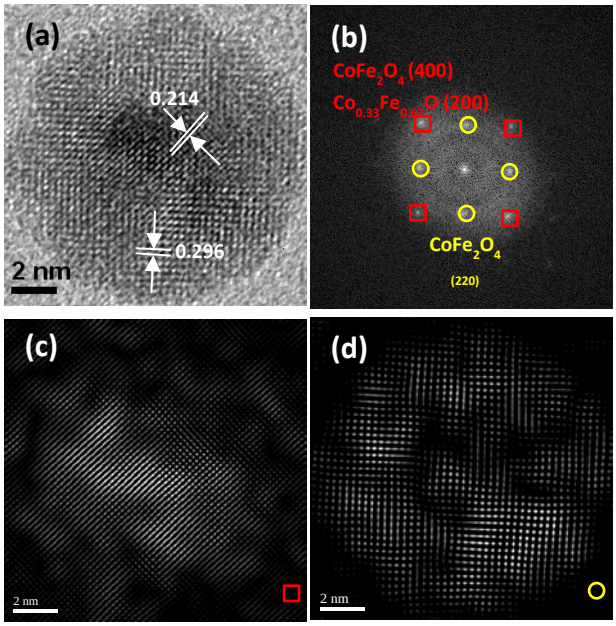

Fig. S5. The electron diffraction pattern of a single particle in the 20-h sample was used to further analyze the phase distribution.

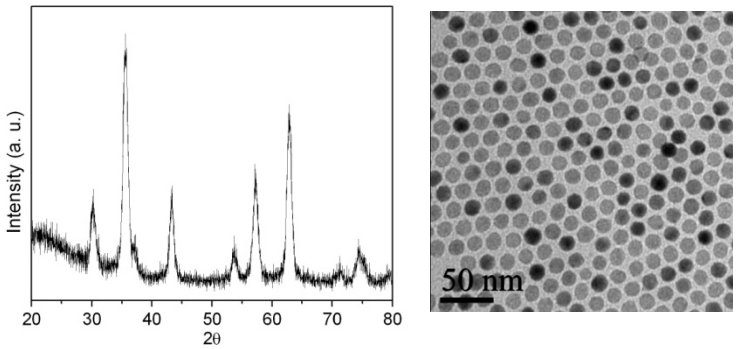

Fig. S6. XRD and TEM of the fully oxidized 12.5 nm $CoFe_2O_4$ sample.

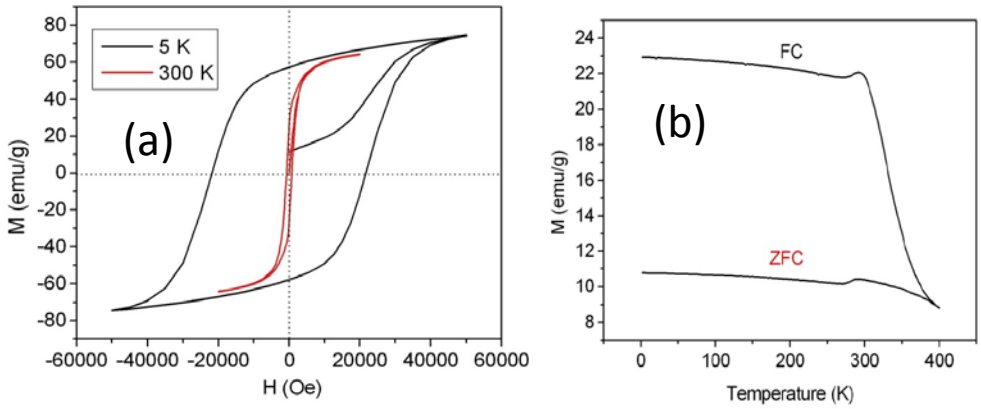

Fig. S7. The hysteresis loop (a) and temperature-dependent magnetization curve (b) of the fully oxidized 12.5 nm $CoFe_2O_4$ sample.

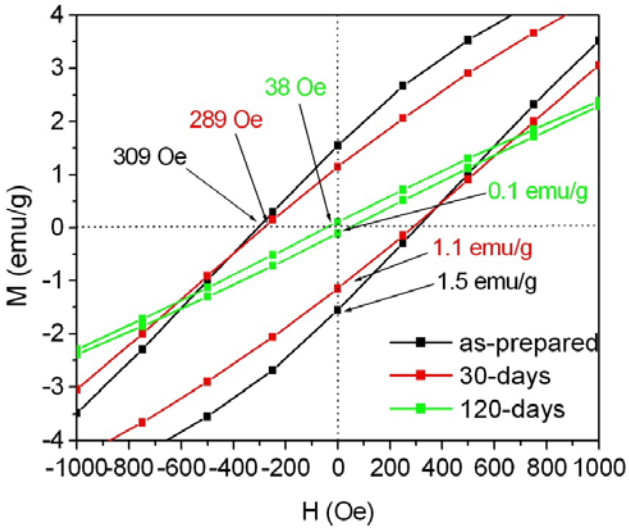

Fig. S8. The 300-K hysteresis loops of all three ambient oxidation samples show strong H_C and M_r.

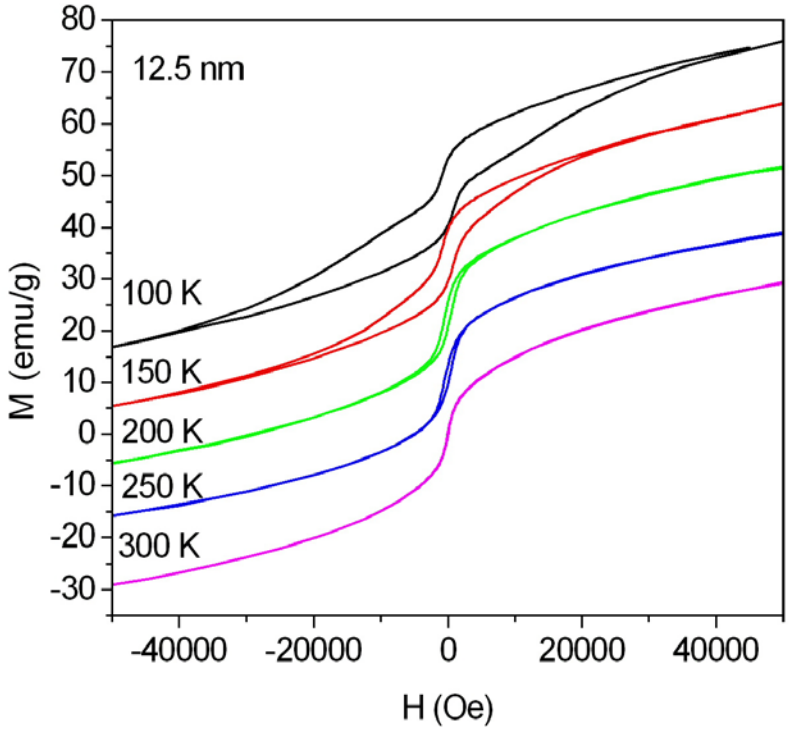
12.5 nm
100 K
150 K
200 K
250 K
300 K
M (emu/g)
H (Oe)
80
70
60
50
40
30
20
10
0
-10
-20
-30
-40000
-20000
0
20000
40000

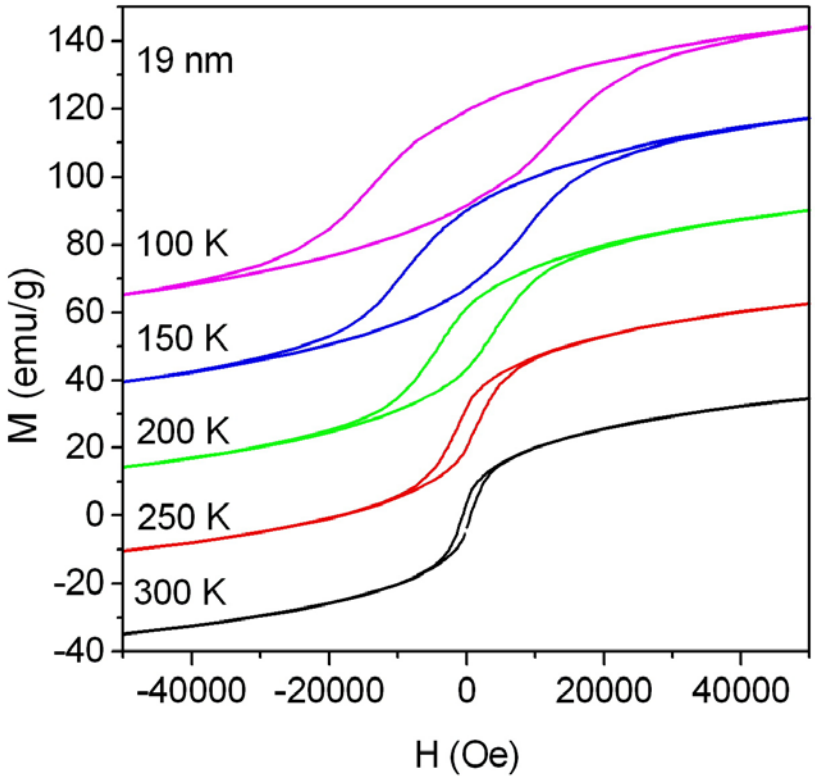
19 nm
100 K
150 K
200 K
250 K
300 K
M (emu/g)
H (Oe)
140
120
100
80
60
40
20
0
-20
-40
-40000
-20000
0
20000
40000

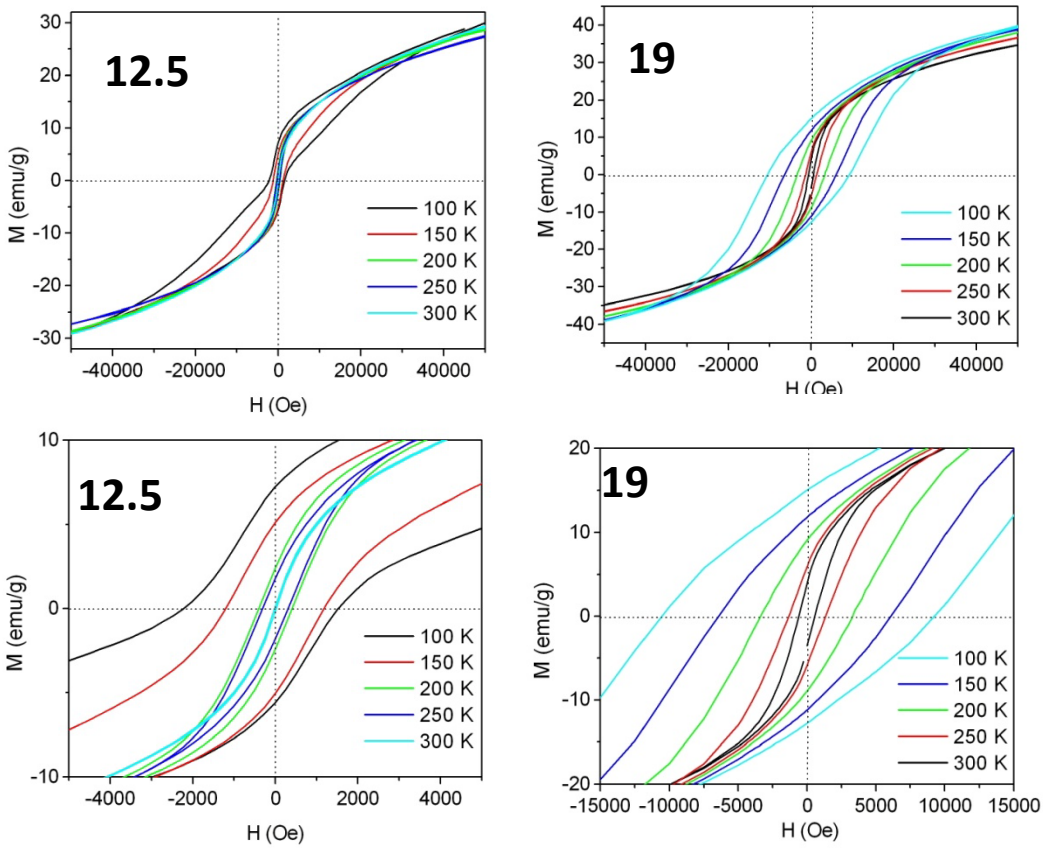

Fig. S9. The temperature-dependent hysteresis loops under FC (5 T) conditions at temperatures ranging from 100 K to 300 K with a step size of 50 K for products of 20-h expedited oxidation samples.

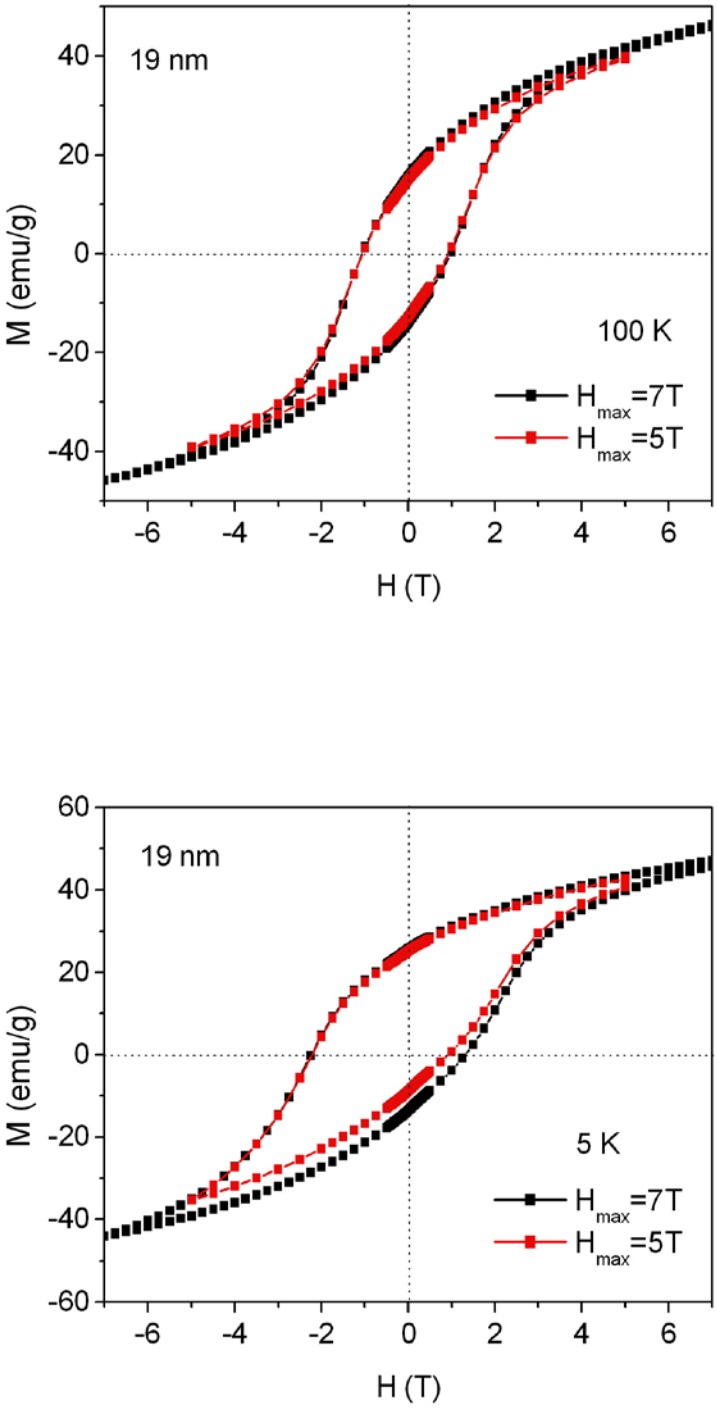

Figure S10. The hysteresis loops under FC (5 T and 7T) conditions at 5K and 100 K show similar H_{irr} indicating the magnetic field 5 T is sufficient to saturate the shell even at low temperature.